

Jay Spampanato and Istvan Mody

J Neurophysiol 98:96-104, 2007. First published May 2, 2007; doi:10.1152/jn.00188.2007

You might find this additional information useful...

This article cites 32 articles, 16 of which you can access free at:

<http://jn.physiology.org/cgi/content/full/98/1/96#BIBL>

Updated information and services including high-resolution figures, can be found at:

<http://jn.physiology.org/cgi/content/full/98/1/96>

Additional material and information about *Journal of Neurophysiology* can be found at:

<http://www.the-aps.org/publications/jn>

This information is current as of April 18, 2008 .

Spike Timing of Lacunosom-Moleculare Targeting Interneurons and CA3 Pyramidal Cells During High-Frequency Network Oscillations In Vitro

Jay Spampanato and Istvan Mody

Department of Neurology, David Geffen School of Medicine, University of California, Los Angeles, California

Submitted 19 February 2007; accepted in final form 25 April 2007

Spampanato J, Mody I. Spike timing of lacunosom-moleculare targeting interneurons and CA3 pyramidal cells during high-frequency network oscillations in vitro. *J Neurophysiol* 98: 96–104, 2007. First published May 2, 2007; doi:10.1152/jn.00188.2007. Network activity in the 200- to 600-Hz range termed high-frequency oscillations (HFOs) has been detected in epileptic tissue from both humans and rodents and may underlie the mechanism of epileptogenesis in experimental rodent models. Slower network oscillations including theta and gamma oscillations as well as ripples are generated by the complex spike timing and interactions between interneurons and pyramidal cells of the hippocampus. We determined the activity of CA3 pyramidal cells, stratum oriens lacunosum-moleculare (O-LM) and s. radiatum lacunosum-moleculare (R-LM) interneurons during HFO in the in vitro low-Mg²⁺ model of epileptiform activity in *GIN* mice. In these animals, interneurons can be identified prior to cell-attached recordings by the expression of green-fluorescent protein (GFP). Simultaneous local field potential recordings from s. pyramidale and on-cell recordings of individual interneurons and principal cells revealed three primary firing behaviors of the active cells: 36% of O-LM interneurons and 60% of pyramidal cells fired action potentials at high frequencies during the HFO. R-LM interneurons were biphasic in that they fired at high frequency at the beginning of the HFO but stopped firing before its end. When considering only the highest frequency component of the oscillations most pyramidal cells fired on the rising phase of the oscillation. These data provide evidence for functional distinction during HFOs within otherwise homogeneous groups of O-LM interneurons and pyramidal cells.

INTRODUCTION

Hippocampal synchronized network activity is associated with well-defined behavioral states and with the development of seizures. Slow oscillations (5–10 Hz, theta) are associated with active exploration and rapid-eye-movement (REM) sleep (Buzsaki 2002; O'Keefe and Nadel 1978), whereas faster (30–100 Hz, gamma) activity is associated with awake, attentive behavior and REM sleep (Buzsaki et al. 2003; Fries et al. 2001; Gray 1994; Singer 1993). The very fast (100- to 200-Hz; ripples) activity superimposed on sharp waves lasting 50–100 ms is correlated with memory formation during slow-wave sleep and awake immobility (Ylinen et al. 1995). Ultrafast oscillations (200–600 Hz) termed high-frequency oscillations (HFOs) have been detected in epileptic tissue of humans and rodents (Bragin et al. 1999a,b, 2002) and may underlie epileptogenesis in rodent models (Bragin et al. 2004).

Theta, gamma, and ripple oscillations are generated by the complex spike timing and interactions between interneurons and pyramidal cells of the hippocampus (Gloveli et al. 2005;

Hajos et al. 2004; Klausberger et al. 2003; Mann et al. 2005). The O-LM interneurons provide theta rhythm inhibitory feedback (Klausberger et al. 2003; Gloveli et al. 2005) and fire phase locked to the gamma rhythm (Hajos et al. 2004). In contrast, stratum radiatum lacunosum-moleculare (R-LM) interneurons fire with no specificity during gamma oscillations (Hajos et al. 2004). S. oriens LM (O-LM) cells fire at high frequencies under artificial stimulation (Aradi and Maccaferri 2004; Fujiwara-Tsukamoto et al. 2004; Gloveli et al. 2005; Zhang and McBain 1995), and they respond specifically to high-frequency synaptic input (Pouille and Scanziani 2004), but they are completely silent during ripple activity (Klausberger et al. 2003). Moreover, O-LM interneurons fire only at low frequencies while phase-locked to theta (Klausberger et al. 2003) and gamma oscillations (Hajos et al. 2004) possibly due to a lack of high-frequency input from pyramidal cell collaterals. However, pyramidal cells fire action potentials at high frequencies in some in vitro models of epileptiform activity (Aradi and Maccaferri 2004; Dzhala and Staley 2004; Laszotoczi et al. 2004; Mody et al. 1987), suggesting a possible role for O-LM cells in HFO.

To study the activity of pyramidal cells and O- and R-LM interneurons during HFO, we utilized the in vitro low-Mg²⁺ model of epileptiform activity (Jones and Heinemann 1988; Mody et al. 1987; Walther et al. 1986) and the genetic expression of green-fluorescent protein (GFP) in *GIN* mice to identify interneurons prior to cell-attached recordings. About 96% of the GFP-positive cells in the CA3 of *GIN* mice express somatostatin and mGluR1 α (Oliva et al. 2000), both markers of O-LM cells (Somogyi and Klausberger 2005). Further anatomical analysis of the GFP-positive cells showed them to be O- and R-LM interneurons based on their dendritic morphology and axonal targeting (Oliva et al. 2000). Following simultaneous field recordings from s. pyramidale and single-unit recordings of individual interneurons and principal cells, we found three primary firing behaviors: 36% of the O-LM interneurons and 60% of the pyramidal cells fired action potentials at high frequencies during HFO, whereas the remainder were silent during the HFOs. R-LM interneurons were biphasic in that they fired at high frequency at the beginning of the HFO but stopped firing before its end. When considering only the early (first 30 ms) and typically the highest-frequency component of the oscillations most pyramidal cells fired with phase association correlated with the rising phase of the oscillation.

Address for reprint requests and other correspondence: I. Mody, UCLA, Neurology NRB1 Rm. 575D, 635 Charles E. Young Dr. South, Los Angeles, California 90095-7335 (E-mail: Mody@ucla.edu).

The costs of publication of this article were defrayed in part by the payment of page charges. The article must therefore be hereby marked "advertisement" in accordance with 18 U.S.C. Section 1734 solely to indicate this fact.

METHODS

Slice preparation

Slices were obtained from adult (2–4 mo old) male *GIN* mice (Oliva et al. 2000) originally purchased from The Jackson Laboratory (Bar Harbor, ME) and bred at the UCLA Division of Laboratory Animal Medicine. In accordance with the UCLA Chancellor's Animal Research Committee approved protocol, the mice were anesthetized with halothane prior to decapitation. Brains were quickly removed and placed into ice-cold normal artificial cerebrospinal fluid (ACSF) containing (in mM) 126 NaCl, 2.5 KCl, 2 CaCl₂, 2 MgCl₂, 1.25 NaHPO₄, 26 NaHCO₃, 10 D-glucose, 1.5 glutamine, and 1.5 Na-pyruvate with pH 7.3–7.4 when bubbled with 95% O₂-5% CO₂. Normal ACSF was supplemented with 3 mM kynurenic acid (Spectrum Chemical Manufacturing, Gardena, CA) for the duration of the cutting procedure. Slices (350 μm thick) were cut in the horizontal orientation using a Leica VT1000S Vibratome, (Leica Microsystems, Wetzlar, Germany). The slices were then transferred to an interface style holding chamber containing normal ACSF at 32°C and allowed to recover for ≥1 h prior to experimentation.

Local field potential and cell-attached recordings

Slices were placed in a submerged recording chamber modified to promote laminar flow and perfused at >8 ml/min with an extracellular recording solution containing (in mM) 126 NaCl, 5 KCl, 1.2 CaCl₂, 0.05 MgCl₂, 1.25 NaHPO₄, 26 NaHCO₃, 10 D-glucose, 1.5 glutamine, and 1.5 Na-Pyruvate. The recording solution was aerated with 95% O₂-5% CO₂, and the bath temperature was maintained at 34°C. Under these conditions, recordings in the CA3 pyramidal cell layer showed epileptiform bursting to occur within minutes of submersion in the recording solution. To consistently obtain spontaneous oscillations, it was necessary to fit the chamber with small plastic fibers fixed parallel to the direction of solution flow thereby elevating the slices off the glass coverslip. Microelectrodes (1–5 MΩ when filled) were pulled from 7740 glass (Garner Glass, Claremont, CA) and filled for field recordings with the extracellular solution and for cell-attached recordings with 126 mM NaCl and 10 mM HEPES adjusted to pH 7.2. The field potential recordings were obtained through an electrode placed in the s. pyramidale of CA3 while simultaneous single-unit recordings were made with a second electrode positioned <400 μm away from the field electrode. The recordings presented here were taken primarily from the subregion CA3c and CA3b however similar activity was observed in CA3a. The firing patterns of single cells were recorded in the cell-attached loose-patch configuration from visually identified pyramidal cells and green fluorescent interneurons. All recordings were obtained DC in the current-clamp configuration (*I* = 0) using the Axon Instruments MultiClamp 700A (Molecular Devices, Sunnyvale, CA) at 10-kHz sampling frequency through a 3-kHz low-pass filter with EVAN data collection software (in house).

Data analysis

Analysis was completed using both EVAN and Igor software (WaveMetrics, Lake Oswego, OR). Bursts were detected on their negative field spike. This was used to define the start of the oscillations. In all cases, the detected points that began the negative field spike were subsequently labeled as *time 0* for alignment and quantification purposes. An interburst interval histogram was generated for each recording (bin width = 0.1 s). A Gaussian was fit to the histogram to determine the average interburst interval and its SD within the recording. Individually detected action potentials were then assigned to a burst if they occurred within 1–3 SDs before to 0.4 s after the start of the burst (4-fold longer than the average burst duration). A raster plot was generated by plotting the action potential

time relative to the start of each detected burst. To determine the action potential frequency, the time leading up to a burst was binned at 100 ms, and the time during and after a burst was binned at 20 ms. The number of action potentials in each bin was counted and the values and SDs were then scaled to 1 s to generate the average firing frequency (s⁻¹). Wigner transforms of field oscillations band-pass filtered between 100 and 1,000 Hz were calculated using the built-in function of Igor. In all cases, the filtered data were phase adjusted to eliminate errors introduced during the filtering. For cells that fired during the HFO, phase association was determined using the Hilbert transform. Action potentials that occurred during the first 30 ms of the oscillations, the time period during which the strongest and highest frequency activity was observed, were then assigned an angle based on the corresponding phase using the built-in phase-corrected functions of IGOR. Circular statistics were used to calculate the mean angle and vector length for each cell and Rayleigh's test was applied to determine the significance of the directionality of firing. More specifically the mean angle is determined by first calculating the mean sine (\bar{s}) and the mean cosine (\bar{c}) for each cell as follows

$$\bar{s} = \frac{\sum \sin(a)}{n}$$

$$\bar{c} = \frac{\sum \cos(a)}{n}$$

where *a* is the angle for each action potential and *n* is the total number of angles. Then the mean angle ($\bar{\theta}$) is

$$\bar{\theta} = \arctan\left(\frac{\bar{s}}{\bar{c}}\right)$$

The mean vector length (*r*) is then

$$r = \sqrt{(\bar{s})^2 + (\bar{c})^2}$$

The polar plots displayed in Figs. 8B and 9B are circular histograms of the probability of action potential firing at each phase of the oscillation.

RESULTS

HFOs in the submerged chamber.

Perfusion of a Mg²⁺-free or low-Mg²⁺ recording solution has been shown previously to result in regular epileptiform activity in the CA1 and CA3 regions of the hippocampus in vitro (Jones and Heinemann 1988; Mody et al. 1987; Walther et al. 1986). Although the activity was described as robust and reproducible, all of these studies used an interface-style recording chamber that cannot be combined with the visualization and fluorescent identification of individual interneurons for single-cell recordings. By modifications of the recording chamber (see METHODS) and increasing the rate of perfusion to >8 ml/min similar to what was reported recently to elicit stable gamma oscillations under similar conditions (Hajos et al. 2004; Mann et al. 2005), we were able to reliably reproduce regular epileptiform activity in the submerged chamber with no requirement for additional tetanization or drug application (Fig. 1). Figure 1A illustrates 60 s of a typical field recording from the CA3 pyramidal cell layer of a regularly bursting slice. The expanded burst demonstrates a standard field recorded waveform: each burst begins with a large fast negative field deflection followed by a slower, larger positive potential that on return to baseline and overshoots to go negative again before settling more slowly back to baseline (Fig. 1A, *middle*). The

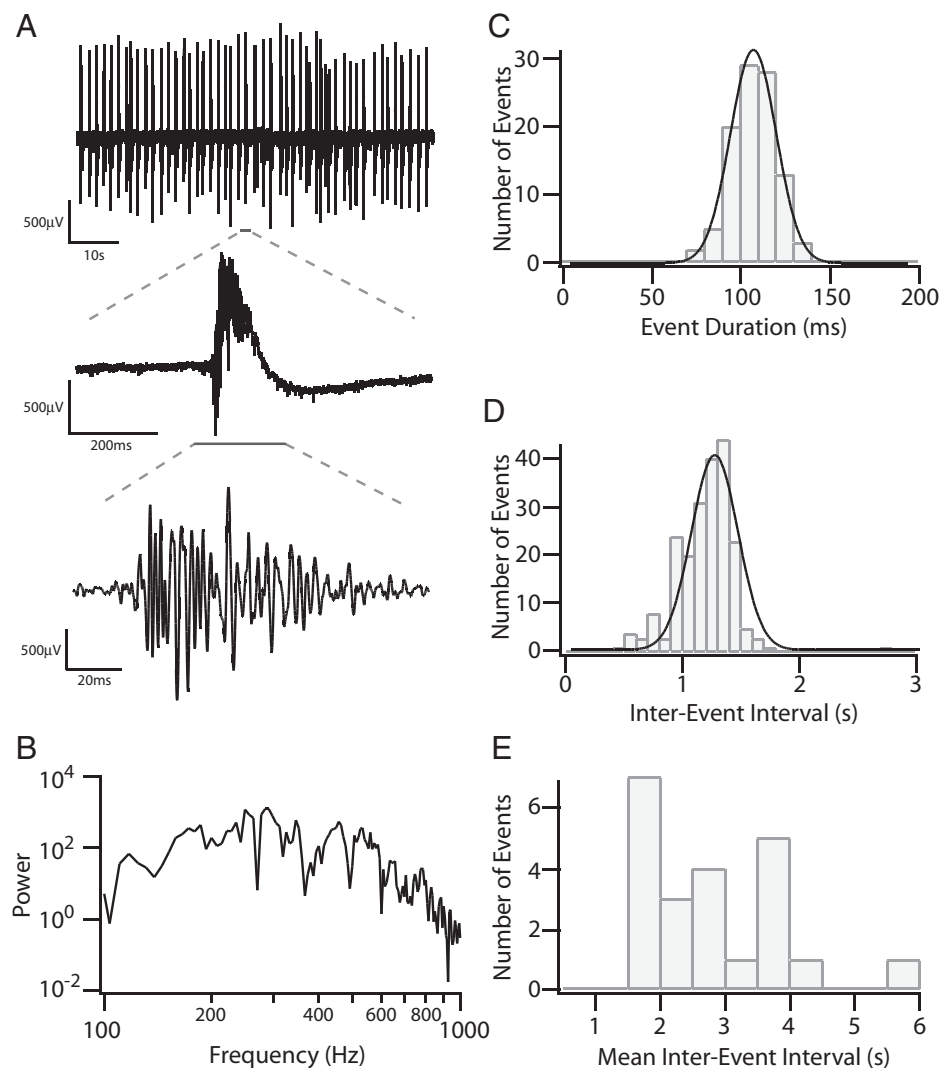


FIG. 1. Low Mg^{2+} induced spontaneous high-frequency activity in CA3 stratum pyramidale recorded in a submerged chamber. *A, top*: field recording from s. pyramidale of CA3 after perfusion of artificial cerebrospinal fluid (ACSF) containing 0.05 mM Mg^{2+} . Field activity could be observed within minutes of submersion in the recording media. *Middle*: 1 burst is expanded to illustrate the typical field waveform. *Bottom*: expanded high-frequency oscillation (HFO) is shown band-pass filtered between 100 and 1,000 Hz. *B*: fast Fourier transform of the expanded HFO showing high power in the 200- to 600-Hz range. *C* and *D*: histograms of the duration (*C*) and inter-event intervals (*D*) of the first 100-200 HFOs of the recording shown in *A*. The event duration histogram is fit with a Gaussian centered at 108.1 ± 12.9 (SD) s. The interevent interval histogram is fit with a Gaussian centered at 1.2 ± 0.2 s. *E*: mean interburst interval histogram of 22 slices shows that the time between the bursts was variable, ranging between 1 and 4 s for 91% of the slices (20/22).

high-frequency oscillations lasted on average for 108 ms (Fig. 1C) as can be seen in the expanded trace band-pass filtered between 100 and 1,000 Hz (Fig. 1A, *bottom*). Individual epileptiform bursts consist of a complex and variable assortment of high-frequency activity in the fast ripple band of 200–600 Hz demonstrated by the fast Fourier transform (Fig. 1B) of the oscillation shown in Fig. 1A. This slice displayed continuous HFOs with an interburst interval of ~ 1.3 s (Fig. 1D). For all experiments, the average interburst interval was 2.3 ± 0.2 (SE) s ($n = 22$) with a range between 1.1 and 5.2 s (Fig. 1E). Within a given slice, the bursts occurred regularly for up to several hours with little change.

Spike timing of s. lacunosum-moleculare targeting interneurons during HFO

To determine the single-unit firing patterns of principal cells and interneurons that generate the high-frequency field oscillations, we performed simultaneous noninvasive loose-patch cell-attached recordings from visually identified pyramidal cells and GFP-expressing somatostatin O- and R-LM interneurons in the CA3 region of the hippocampus of *GIN* mice. O- and R-LM interneurons were scattered throughout each slice and were easily identifiable due to the high expression of GFP (Fig. 2). These cells were previously characterized and concluded to be exclusively somatostatin-expressing, mGluR1 α -

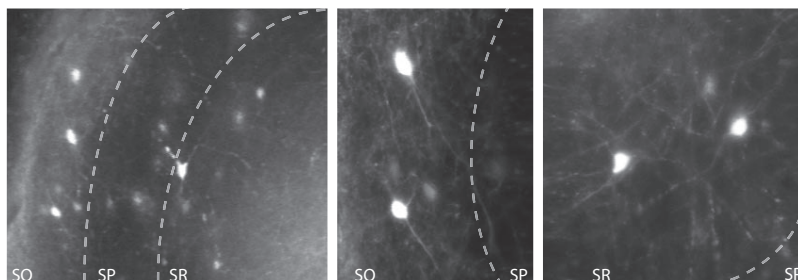


FIG. 2. Green-fluorescent protein (GFP)-expressing interneurons in the CA3 region of the hippocampus. *Left*: $\times 10$ magnification of the CA3 region of a *GIN* mouse. GFP-expressing cells can be seen throughout the 3 layers: s. oriens (SO), s. pyramidale (SP), and s. radiatum (SR). *Middle*: higher magnification ($\times 40$) of 2 interneurons in oriens demonstrating easily identifiable s. oriens lacunosum-moleculare (O-LM) cell bodies and proximal dendrites. *Right*: higher magnification ($\times 40$) of 2 interneurons in the s. radiatum. S. radiatum LM (R-LM) cell somata were typically small.

expressing, s. lacunosum-moleculare targeting interneurons with dendritic arbors consistent with O- or R-LM interneurons (Oliva et al. 2000). We observed a sparse and separated cellular distribution through out the hippocampus similar to that described by Oliva et al. (2000).

The majority of R-LM interneurons (19/23) and approximately half of the pyramidal cells (14/29) and O-LM interneurons (12/26) were found to be inactive in the low-Mg²⁺ recording solution. Inactivity was defined as failure to fire a single action potential over a period of several minutes while the CA3 region was observed to be actively bursting. The mechanism of inactivity cannot be defined through means of loose-patch recordings. It remains possible that these cells were disconnected from the network through the processing of the tissue for in vitro slice recordings. Another possibility stems from the use of a low-Mg²⁺ and 5 mM K⁺ ACSF solution, which could have shifted some pyramidal cells and O- or R-LM interneurons into depolarization block that could have occurred through activation of *N*-methyl-D-aspartate (NMDA) or mGluR1 α receptors on O-LM-interneurons (Baude et al. 1993). Depolarization block has been shown to be an important component of O-LM interneuron activity in much longer seizure-like events in the CA1 region (Ziburkus et al. 2006). Finally, it is likely that this inactivity represents one aspect of cellular assembly into functional units during HFOs. It is generally considered to be the case that higher-frequency oscillations are the result of smaller numbers of participating cells in a given assembly (Buzsaki and Draguhn 2004). The focus of this study was to determine the activity of cells that might contribute to the generation of hippocampal high-frequency oscillations, and therefore from this point on, we consider only the active cells in our analysis. In all experiments, the recorded cells never fired action potentials at the 200- to 600-Hz frequency of the field oscillations.

Based on their firing properties during the HFO the active O-LM interneurons fell into two groups. The first group, representing 36% of active O-LM interneurons, fired rhythmically at an average basal rate of 16 Hz between bursts and increased to an average instantaneous frequency of 183 Hz simultaneous with the start of the oscillation (Fig. 3). These cells exhibited some spike-frequency adaptation but were able to maintain very high-firing rates during the HFO and on average, higher than basal firing rates for ≤ 200 ms from the end of the HFO. This activity is clearly illustrated by both the cell-attached recording (Fig. 3B) and the raster plot of 100 sequential bursts (Fig. 3C). The simultaneous field recording and Wigner transform are included for comparison of the HFO duration, frequency, and timing with the cell activity (Fig. 3A).

The second group, representing 63% of active O-LM interneurons, fired at a significantly higher average basal rate of 30 Hz in-between bursts (Student's *t*-test, $P < 0.01$) but abruptly stopped firing at the beginning of the epileptiform burst and remained silent for the duration of the HFO (Fig. 4). These cells then slowly returned to their basal firing rate requiring >300 ms from the end of the HFO to fully recover (Fig. 4, B and C). The simultaneously recorded field oscillation, band-pass filtered inset, and Wigner transforms are included for comparison of the timing of the single-cell activity with the network activity (Fig. 4A). This group of O-LM cells was never observed to fire at the extreme high frequencies reported for the previous group.

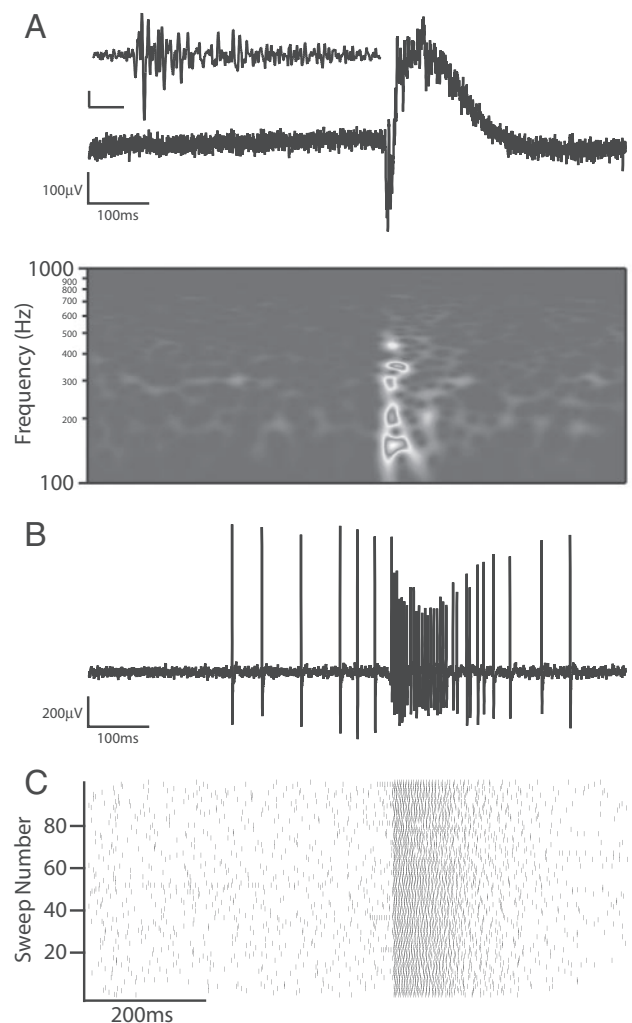


FIG. 3. Increased firing of O-LM interneurons during high-frequency oscillations. *A*, top: field recording from s. pyramidale of CA3 after perfusion of 0.05 mM Mg²⁺ ACSF. *Inset*: expanded trace of the HFO band-pass filtered between 100 and 1,000 Hz. Scale bars are 50 μ V and 25 ms. *Bottom*: Wigner transform of the band-pass filtered field recording demonstrating the frequency spectra of the oscillations present during the HFO. *B*: loose-patch cell-attached recording during the field burst illustrated in *A* from a visually identified GFP-expressing O-LM interneuron located <300 μ m away from the field electrode. Some basal firing activity prior to the HFO is followed by an immediate increase in firing simultaneous with the start of the HFO. *C*: raster plot of action potential firing during 100 sequential bursts illustrates the consistency of this pattern of activity over time.

R-LM interneurons were far less likely to be active in the low-Mg²⁺ recording solution than both O-LM interneurons and pyramidal cells. All of the R-LM interneurons that were active (4/4) maintained the highest average basal firing rate at 39 Hz (significantly faster than both groups of O-LM interneurons, Student's *t*-test, $P < 0.05$). Each active R-LM interneuron increased firing to an average spontaneous rate of 135 Hz for a brief period simultaneous with the beginning of the field oscillations but rapidly slowed before the end of the epileptiform burst (Fig. 5). In contrast to the O-LM interneurons that stopped firing during the HFO, R-LM interneurons quickly returned to their basal firing rate of 39 Hz within 50 ms after the end of the HFO. The raw trace shown depicts the irregular basal firing of the R-LM interneurons with no discernable change in behavior immediately prior to the field oscillation

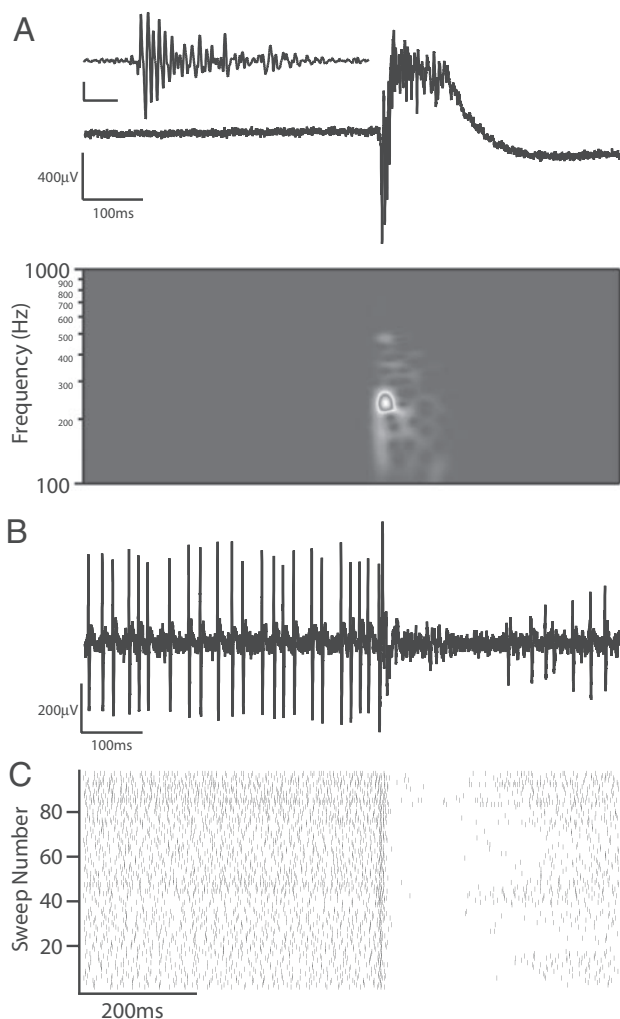


FIG. 4. Decreased firing of O-LM interneurons during HFOs. *A*, *top*: field recording from s. pyramidale of CA3 after perfusion of 0.05 mM Mg^{2+} ACSF. *Inset*: burst in *A* band-pass filtered between 100 and 1,000 Hz. Scale bars are 200 μ V and 25 ms. *Bottom*: Wigner transform of the band-pass-filtered field recording demonstrating the frequency spectra of the oscillations present during the HFO. *B*: loose-patch cell-attached recording during the field burst illustrated in *A* from a visually identified GFP expressing O-LM interneuron located $<300 \mu$ m away from the field electrode. High basal firing activity can be seen prior to the HFO followed by an immediate cessation of firing simultaneous with the start of the HFO. *C*: raster plot of action potential firing during 100 sequential bursts illustrates the consistency of this pattern of activity over time. This cell sometimes fired 1 or 2 action potentials in rapid succession just after the negative field spike which can be seen in the dark band of the raster plot.

(Fig. 5, *A* and *B*). The raster plot demonstrates the consistency of this activity for 80 sequential bursts (Fig. 5*C*).

Spike timing of CA3 pyramidal cells during HFO

The basal firing rate of all active pyramidal cells was typically only a few hertz. Similar to the O-LM interneurons, active pyramidal cells could be classified into two groups based only on their activity during the HFO. The first group, representing 60% of the active pyramidal cells, fired at very high frequencies simultaneous with the HFO (Fig. 6). In step-wise fashion, these pyramidal cells increased firing to an average instantaneous rate of 154 Hz and exhibited significant spike-

frequency adaptation throughout the duration of the field oscillation (Fig. 5, *A* and *B*). In contrast to the high-frequency firing observed in O-LM interneurons, pyramidal cells returned to their basal firing rate of only a few hertz coincident with the completion of the HFO; that is, they did not continue to fire at a higher than basal rate in the absence of a detectable field oscillation. The raster plot demonstrates the sporadic firing of pyramidal cells leading up to each burst and the decline in frequency during the HFOs (Fig. 5*C*).

The second group, representing 40% of active pyramidal cells, similarly displayed a low basal firing rate between bursts; however they stopped firing during the field oscillations (Fig. 7). In contrast to the O-LM interneurons that stopped firing during HFOs, the pyramidal cells exhibited a unique firing

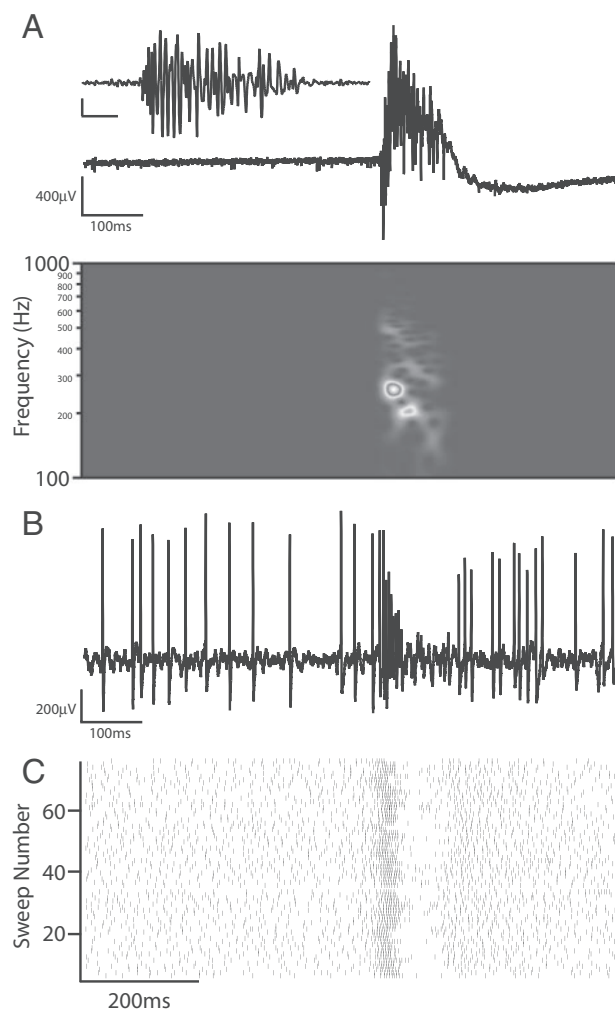


FIG. 5. Biphasic firing of R-LM interneurons during HFOs. *A*, *top*: field recording from s. pyramidale of CA3 after perfusion of 0.05 mM Mg^{2+} ACSF. *Inset*: burst in *A* band-pass filtered between 100 and 1,000 Hz. Scale bars are 200 μ V and 25 ms. *Bottom*: Wigner transform of the band-pass filtered field recording demonstrating the frequency spectra of the oscillations present during the HFO. *B*: loose-patch cell-attached recording from a visually identified GFP expressing R-LM interneuron during the field burst illustrated in *A* located $<300 \mu$ m away from the field electrode. The irregular basal firing activity (39 Hz) prior to the HFO is increased dramatically coincident with the start of the HFO. R-LM interneurons fired a few action potentials in rapid succession before likely entering into depolarization block, from which they recovered immediately following the HFO. *C*: raster plot of action potential firing during 80 sequential bursts illustrates the consistency of this pattern of activity over time.

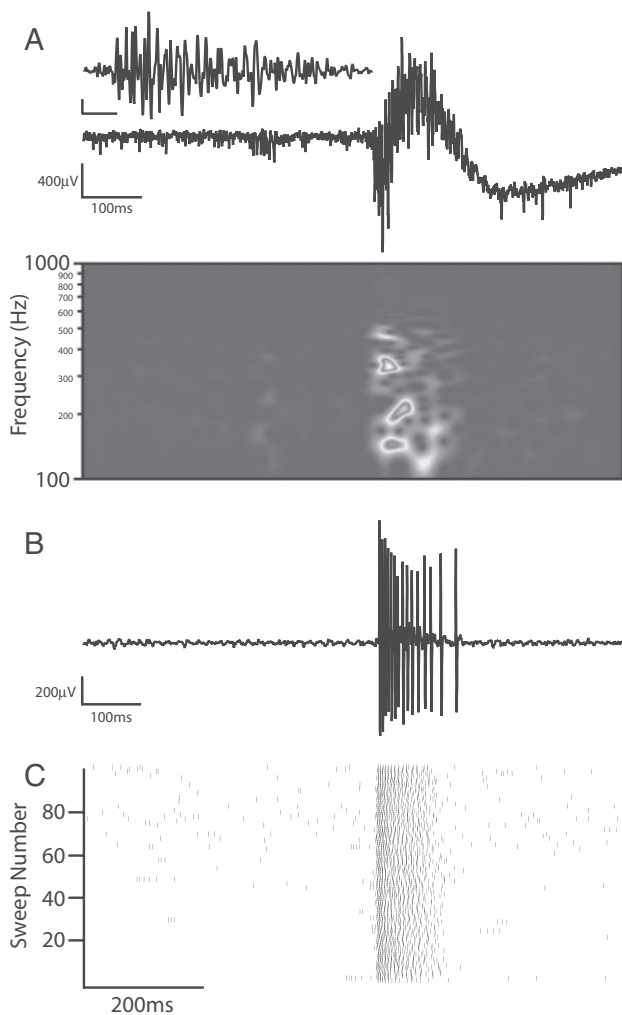


FIG. 6. Increased firing of a CA3 pyramidal cell during HFOs observed in 9 of 15 pyramidal cells. *A, top*: field recording from s. pyramidale of CA3 bathed in 0.05 mM Mg^{2+} ACSF. *Inset*: illustrated burst band-pass filtered between 100 and 1,000 Hz. Scale bars are 200 μV and 25 ms. *Bottom*: Wigner transform of the band-pass filtered field recording demonstrating the frequency spectra of the oscillations present during the HFO. *B*: loose-patch cell-attached recording from a visually identified CA3 pyramidal cell $<100 \mu m$ from the field electrode. This trace demonstrates no basal firing activity prior to the HFO followed by an immediate increase in firing simultaneous with the start of the HFO. *C*: raster plot of action potential firing during 100 sequential HFOs illustrates the consistency of this pattern of activity over time as well as the intermittent low-frequency inter-event firing during some sweeps.

pattern in that they specifically fired one or a few action potentials tightly synchronous with the negative field deflection signifying the start of the epileptiform burst (Fig. 7, *A* and *B*). The raster plot again demonstrates the sporadic firing nature of these pyramidal cells during the interevent interval, the precise firing of a few action potentials at the start of the epileptiform burst, and the consistent lack of firing during the HFO (Fig. 7*C*). It is important to note that all of the active pyramidal cells demonstrated some level of sporadic firing between oscillations regardless of their behavior during the HFOs.

Figures 8*A* and 9*A* depict the summarized activity of each individual group described in the preceding text. The light gray area signifies the start and average HFO duration. It is easy to see the contrast in behavior between the two groups of O-LM interneurons and the two groups of pyramidal cells as well as

the biphasic activity of the R-LM interneurons. This figure also depicts the rapid cessation of firing in pyramidal cells compared with the extended activity in the O-LM interneurons that fired at high frequency.

Because each individual HFO typically consisted of multiple bands of high-frequency activity that changed over time, we concentrated only on the first 30 ms to determine if the firing of any of the cells active during the HFO was associated with a specific phase of the oscillation. This duration was long enough to include the highest-frequency and highest-power activity that typically occurred at the start of the HFO. During this time period, the majority of O- and R-LM interneurons did not fire with any specific phase association. This can be seen in the polar histograms depicting their firing behavior (Fig. 8*B*).

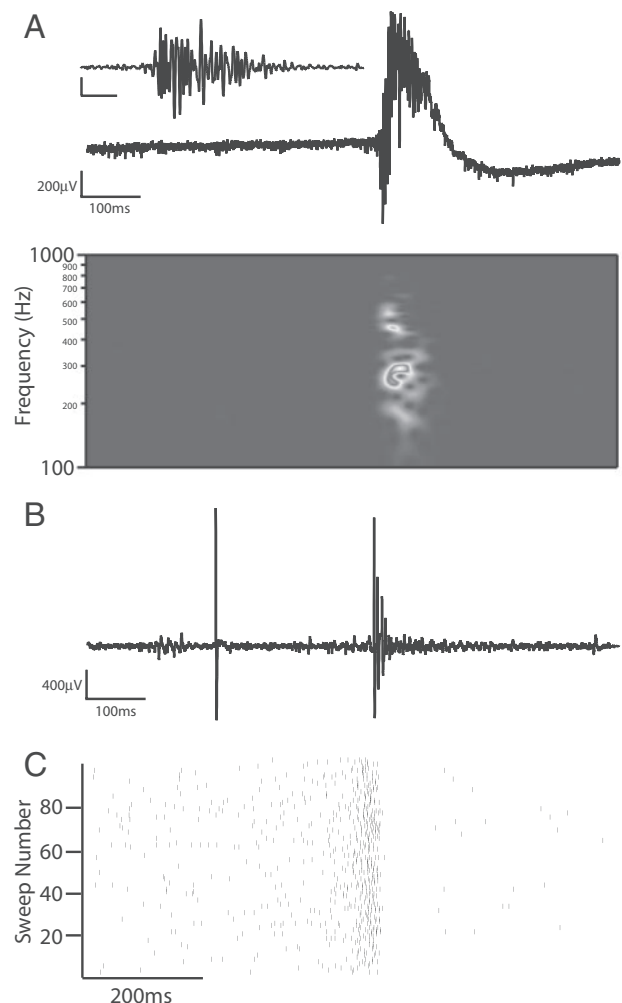


FIG. 7. Decreased firing of a CA3 pyramidal cell during HFOs observed in 6 of 15 pyramidal cells. *A, top*: field recording from the CA3 s. pyramidale in 0.05 mM Mg^{2+} ACSF. *Inset*: burst in *A* is shown band-pass filtered between 100 and 1,000 Hz. Scale bars: 200 μV and 25 ms. *Bottom*: Wigner transform of the band-pass filtered field recording demonstrating the frequency spectra of the oscillations present during the HFO. *B*: loose-patch cell-attached recording from a visually identified CA3 pyramidal cell $<100 \mu m$ from the field electrode. Note the low basal firing activity prior to the HFO followed by the firing of 1–3 precisely timed action potentials simultaneous with the start of the HFO. *C*: raster plot of action potential firing during 100 sequential HFOs illustrates the consistency of this pattern of activity over time. Although this particular pyramidal cell can be seen to increase firing immediately prior to the start of the oscillation this was not seen in the averaged data.

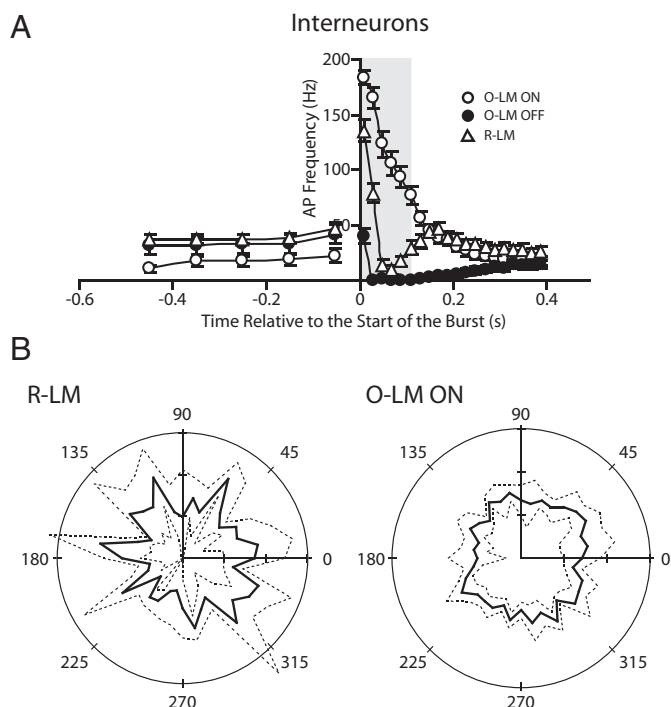


FIG. 8. Average firing rates of O- and R-LM interneurons during HFO. *A*: average firing rates of the three groups of interneurons categorized by their activity during the HFO. To calculate the specific rate of firing of each cell, the time prior to each HFO was binned into periods of 100 ms while the time during and after each HFO was binned into 20 ms periods. Action potentials were then summed per bin and averaged across the cells within each group. These data were then scaled to obtain the number of action potentials per second (Hz). The area shaded in gray represents the start and duration of an average HFO burst. Error bars are SDs. (*n* for each group: O-LM ON = 4, O-LM OFF = 7, R-LM = 4). *B*: spike probability polar histograms were calculated according to the phase of firing for the O-LM ON and R-LM interneurons during the first 30 ms of the corresponding HFOs. —, average data; ---, \pm SD. In each plot the circle maximum probability is 0.06 and the *x* and *y* axes ticks represent probabilities toward the origin of 0.04 and 0.02, the origin is 0

In contrast, during the same period, a majority of pyramidal cells did fire with a phase association corresponding to the rising slope of the oscillation (for 6/9 cells, Rayleigh's test $P < 0.05$ with a mean angle of 125° and a mean vector of 0.08). The polar histogram displays the average phase associated action potential probability of all of the active pyramidal cells (Fig. 9*B*). The raw data demonstrate the phase association of action potential firing (Fig. 9*C*) during the early high-frequency, high-power oscillation. In this example, the first action potential occurred immediately before the start of the HFO. The second through fifth action potentials fired on the rising phase of the 215- to 344-Hz oscillation and the last four action potentials fired out of phase.

DISCUSSION

We have presented here for the first time in adult mice, low- Mg^{2+} -induced HFOs in a submerged hippocampal slice without the requirement of additional pharmacological agents or tetanus to further enhance neuronal excitability. The CA3 region generated spontaneous epileptiform field oscillations in the HFO band of 200–600 Hz repeatedly and reliably at a rate of ~ 0.5 Hz. Once the HFOs were established, cell-attached

recordings were used to determine the activity of CA3 pyramidal cells and two types of interneurons: somatostatin expressing O- and R-LM interneurons. During epileptiform bursts, active pyramidal cells were found to fire either at high frequencies on average 150 Hz or just one to three action potentials simultaneous with the start of the field oscillation. Similarly active O-LM interneurons fired either at high frequencies on average 180 Hz or not at all during the field oscillation. All active R-LM interneurons fired in a biphasic

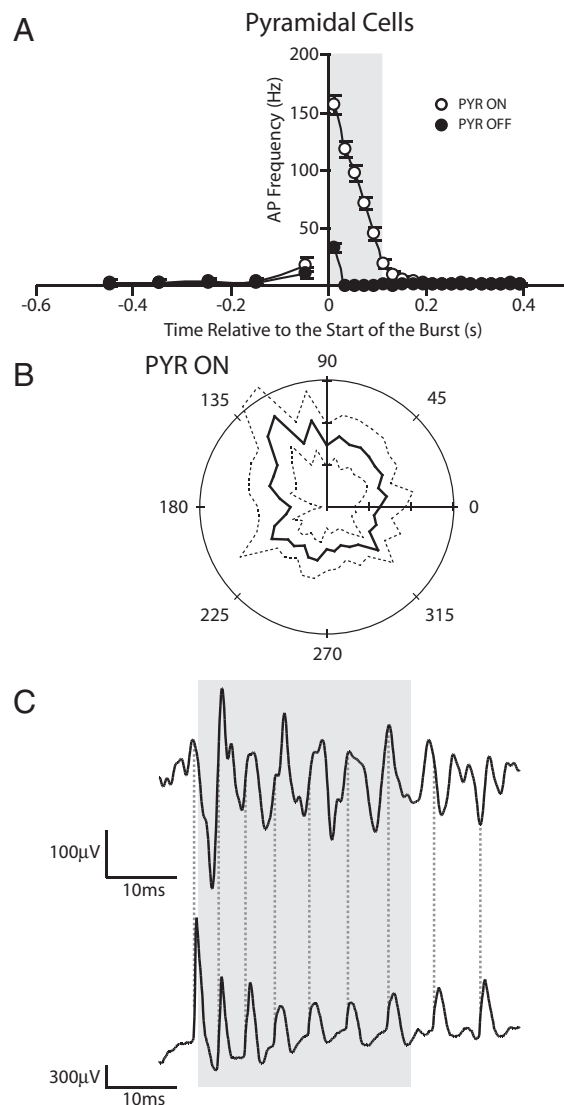


FIG. 9. Average firing rates and phase association of CA3 pyramidal cells during HFO. *A*: average firing rates of the 2 groups of CA3 pyramidal cells categorized by their activity during the HFO were calculated as described in the legend to Fig. 8. (*n* for each group: PYR ON = 9, PYR OFF = 6). *B*: spike probability polar histogram of PYR ON cells calculated according to the phase of firing during the 1st 30 ms of the HFO demonstrates a phase association corresponding to the rising phase of the oscillation with a mean angle of 125° . Six of 9 PYR ON cells demonstrated significant directionality in firing (Rayleigh's test, $P < 0.05$). —, average data; ---, \pm SD. In the plot, the circle maximum probability is 0.06 and the *x* and *y* ticks represent probabilities toward the origin of 0.04 and 0.02, the origin is 0. *C*: CA3 HFO band-pass filtered between 100 and 1,000 Hz (*top*) and the corresponding single-unit recording of 1 phase associated CA3 pyramidal cell (*bottom*). The shaded area, 1st 30 ms of the oscillation with a peak frequency of 215 Hz, which was used for analysis of phase association. During this time, 4 of 6 action potentials were associated with the rising phase of the oscillation.

nature; that is they began to fire at high frequencies on average 140 Hz at the start of the epileptiform bursts but stopped firing halfway through. The field oscillations generated by CA3 in low Mg^{2+} varied at frequencies between 200 and 600 Hz; however, neither the principal cells nor the O-LM/R-LM interneurons fired action potentials at those frequencies. Finally, the firing of the majority of the pyramidal cells could be associated with the rising phase of the early and typically highest frequency portion of the field oscillation.

At all times basal activity between bursts was an order of magnitude higher (16–39 Hz) in the two anatomically defined groups of interneurons compared with the pyramidal cells (1–4 Hz). It is therefore likely that these dendritic targeting interneurons play some role in determining the interevent interval of HFOs. These two unique populations of interneurons are positioned to provide specific inhibition to the excitatory input arriving at the distal dendrites of CA3 pyramidal cells via entorhinal perforant path afferents. R-LM interneurons are likely to provide feed-forward inhibition due to a dendritic arbor primarily confined to strata radiatum and lacunosum-moleculare (Hajos and Mody 1997; Oliva et al. 2000). On the other hand, O-LM interneurons are specifically tuned to provide feed-back inhibition in response to high-frequency input originating from pyramidal cell collaterals (Pouille and Scanziani 2004). Our data further support the likelihood that O-LM interneurons are a critical component in the regulation of CA3 pyramidal cell high-frequency activity. Although there were two functionally different groups of O-LM interneurons and the majority was observed to be inactive during the periods of high-frequency pyramidal cell activity, the inactive group was also already firing action potentials rhythmically at a basal rate of 30 Hz, twice the rate of action potential generation in the group that fired in concert with the high-frequency pyramidal activity. It is possible that the higher basal rate of firing could signify that these O-LM interneurons were already more depolarized and therefore incapable of responding to high-frequency input via pyramidal cell synapses. O-LM interneurons have previously been reported to be completely silent during hippocampal sharp wave ripple (100–200 Hz) oscillations (Klausberger et al. 2003). Likewise, the majority of O-LM interneurons in our study were also silent during the faster low- Mg^{2+} -induced HFOs. In contrast however, we observed tonic firing between oscillations and very high-frequency firing in a number of O-LM interneurons during HFOs consistent with the hypothesis that low- Mg^{2+} -induced HFOs are a better model of pathological high-frequency oscillations than sharp-wave ripples (Bragin et al. 1999a). It is possible this activity signifies a more urgent necessity to inhibit entorhinal input to CA3 during HFOs, whereas doing so during sharp-wave ripples would disrupt the normal operation of the hippocampal-entorhinal circuitry (Chrobak et al. 2000).

The percentage of active pyramidal cells that routinely participate in other fast network oscillations of the hippocampus has been reported to be quite low, ranging from 10 to 22% for sharp-wave ripples and high- K^{+} -induced epileptiform activity, respectively (Dzhala and Staley 2004; Ylinen et al. 1995). In low Mg^{2+} , we found 48% of CA3 pyramidal cells fired spontaneous action potentials. The active pyramidal cells always fired action potentials associated with each HFO. As mentioned in the preceding text, some CA3 pyramidal cells were observed to fire action potentials at very high frequencies

during HFOs. This finding is consistent with previous reports of spontaneous epileptiform activity in CA3 (Aradi and Maccaferri 2004; Dzhala and Staley 2004; Lasztozci et al. 2004; Mody et al. 1987). Of the active pyramidal cells, 60% fired at high frequency during epileptiform bursts and maintained this firing pattern for many minutes, i.e., the duration of the recordings. The remaining 40% fired only one or a few action potentials, suggesting that despite their very similar morphology (Bilkey and Schwartzkroin 1990) there may be at least two functionally different groups of pyramidal cells in CA3. Similar ratios of bursting versus nonbursting CA3 pyramidal cells have been reported after current injection under normal ionic conditions (Bilkey and Schwartzkroin 1990; Masukawa et al. 1982). Although our data suggesting two functional groups of pyramidal cells in CA3 are consistent with these previous findings, we cannot rule out the possibility that the slice technique itself has altered the synaptic inputs to some pyramidal cells causing them to fire fewer action potentials during HFOs. It will be important for future studies to determine whether an individual CA3 pyramidal cell is predetermined to function in one of these two active states (or to be inactive) during spontaneous high-frequency network oscillations in vitro and in vivo or is capable of switching between states in response to changes in incoming synaptic activity or changes in intrinsic properties.

When the full-length HFO was considered for analysis of directional firing, there was no apparent phase association for any of the cells studied here. However, when the analysis was restricted to the early highest power and typically highest frequency portion of the oscillation, a phase association was apparent for the majority of the pyramidal cells that fired during the HFO. During this time, pyramidal cells fired on the rising phase of the oscillation but then continued to fire with no phase association through the end of the oscillation. The loss of phase association could be attributed to their firing at a slower frequency than the field oscillation. Our data also suggest that although the LM targeting interneurons fire during the HFO, they are not the primary interneuronal components of the oscillation.

In conclusion, although high-frequency network oscillations can be recorded throughout CA3 s. pyramidale, our data suggest that this in vitro epileptiform behavior is the result of a smaller subset of synchronized neurons. Our data are also consistent with some functional diversity within otherwise anatomically homogeneous populations of O-LM interneurons and pyramidal cells in the CA3 area.

REFERENCES

- Aradi I, Maccaferri G. Cell type-specific synaptic dynamics of synchronized bursting in the juvenile CA3 rat hippocampus. *J Neurosci* 24: 9681–9692, 2004.
- Baude A, Nusser Z, Roberts JD, Mulvihill E, McIlhinney RA, Somogyi P. The metabotropic glutamate receptor (mGluR1 alpha) is concentrated at perisynaptic membrane of neuronal subpopulations as detected by immunogold reaction. *Neuron* 11: 771–787, 1993.
- Bilkey DK, Schwartzkroin PA. Variation in electrophysiology and morphology of hippocampal CA3 pyramidal cells. *Brain Res* 514: 77–83, 1990.
- Bragin A, Engel J Jr, Wilson CL, Fried I, Buzsaki G. High-frequency oscillations in human brain. *Hippocampus* 9: 137–142, 1999a.
- Bragin A, Engel J Jr, Wilson CL, Fried I, Mathern GW. Hippocampal and entorhinal cortex high-frequency oscillations (100–500 Hz) in human epileptic brain and in kainic acid-treated rats with chronic seizures. *Epilepsia* 40: 127–137, 1999b.

- Bragin A, Mody I, Wilson CL, Engel J Jr.** Local generation of fast ripples in epileptic brain. *J Neurosci* 22: 2012–2021, 2002.
- Bragin A, Wilson CL, Almajano J, Mody I, Engel J Jr.** High-frequency oscillations after status epilepticus: epileptogenesis and seizure genesis. *Epilepsia* 45: 1017–1023, 2004.
- Buzsaki G.** Theta oscillations in the hippocampus. *Neuron* 33: 325–340, 2002.
- Buzsaki G, Buhl DL, Harris KD, Csicsvari J, Czeh B, Morozov A.** Hippocampal network patterns of activity in the mouse. *Neuroscience* 116: 201–211, 2003.
- Buzsaki G, Draguhn A.** Neuronal oscillations in cortical networks. *Science* 304: 1926–1929, 2004.
- Chrobak JJ, Lorincz A, Buzsaki G.** Physiological patterns in the hippocampo-entorhinal cortex system. *Hippocampus* 10: 457–465, 2000.
- Dzhala VI, Staley KJ.** Mechanisms of fast ripples in the hippocampus. *J Neurosci* 24: 8896–8906, 2004.
- Fries P, Reynolds JH, Rorie AE, Desimone R.** Modulation of oscillatory neuronal synchronization by selective visual attention. *Science* 291: 1560–1563, 2001.
- Fujiwara-Tsukamoto Y, Isomura Y, Kaneda K, Takada M.** Synaptic interactions between pyramidal cells and interneurone subtypes during seizure-like activity in the rat hippocampus. *J Physiol* 557: 961–979, 2004.
- Gloveli T, Dugladze T, Saha S, Monyer H, Heinemann U, Traub RD, Whittington MA, Buhl EH.** Differential involvement of oriens/pyramidal interneurons in hippocampal network oscillations in vitro. *J Physiol* 562: 131–147, 2005.
- Gray CM.** Synchronous oscillations in neuronal systems: mechanisms and functions. *J Comput Neurosci* 1: 11–38, 1994.
- Hajos N, Mody I.** Synaptic communication among hippocampal interneurons: properties of spontaneous IPSCs in morphologically identified cells. *J Neurosci* 17: 8427–8442, 1997.
- Hajos N, Palhalmi J, Mann EO, Nemeth B, Paulsen O, Freund TF.** Spike timing of distinct types of GABAergic interneuron during hippocampal gamma oscillations in vitro. *J Neurosci* 24: 9127–9137, 2004.
- Jones RS, Heinemann U.** Synaptic and intrinsic responses of medial entorhinal cortical cells in normal and magnesium-free medium in vitro. *J Neurophysiol* 59: 1476–1496, 1988.
- Klausberger T, Magill PJ, Marton LF, Roberts JD, Cobden PM, Buzsaki G, Somogyi P.** Brain-state- and cell-type-specific firing of hippocampal interneurons in vivo. *Nature* 421: 844–848, 2003.
- Laszotzci B, Antal K, Nyikos L, Emri Z, Kardos J.** High-frequency synaptic input contributes to seizure initiation in the low-[Mg²⁺] model of epilepsy. *Eur J Neurosci* 19: 1361–1372, 2004.
- Mann EO, Suckling JM, Hajos N, Greenfield SA, Paulsen O.** Perisomatic feedback inhibition underlies cholinergically induced fast network oscillations in the rat hippocampus in vitro. *Neuron* 45: 105–117, 2005.
- Masukawa LM, Benardo LS, Prince DA.** Variations in electrophysiological properties of hippocampal neurons in different subfields. *Brain Res* 242: 341–344, 1982.
- Mody I, Lambert JD, Heinemann U.** Low extracellular magnesium induces epileptiform activity and spreading depression in rat hippocampal slices. *J Neurophysiol* 57: 869–888, 1987.
- O'Keefe J, Nadel L.** *The Hippocampus as a Cognitive Map*. Oxford, UK: Oxford Univ. Press, 1978.
- Oliva AA Jr, Jiang M, Lam T, Smith KL, Swann JW.** Novel hippocampal interneuronal subtypes identified using transgenic mice that express green fluorescent protein in GABAergic interneurons. *J Neurosci* 20: 3354–3368, 2000.
- Pouille F, Scanziani M.** Routing of spike series by dynamic circuits in the hippocampus. *Nature* 429: 717–723, 2004.
- Singer W.** Synchronization of cortical activity and its putative role in information processing and learning. *Annu Rev Physiol* 55: 349–374, 1993.
- Somogyi P, Klausberger T.** Defined types of cortical interneurone structure space and spike timing in the hippocampus. *J Physiol* 562: 9–26, 2005.
- Walther H, Lambert JD, Jones RS, Heinemann U, Hamon B.** Epileptiform activity in combined slices of the hippocampus, subiculum and entorhinal cortex during perfusion with low magnesium medium. *Neurosci Lett* 69: 156–161, 1986.
- Ylinen A, Bragin A, Nadasdy Z, Jando G, Szabo I, Sik A, Buzsaki G.** Sharp wave-associated high-frequency oscillation (200 Hz) in the intact hippocampus: network and intracellular mechanisms. *J Neurosci* 15: 30–46, 1995.
- Zhang L, McBain CJ.** Potassium conductances underlying repolarization and after-hyperpolarization in rat CA1 hippocampal interneurons. *J Physiol* 488: 661–672, 1995.
- Ziburkus J, Cressman JR, Barreto E, Schiff SJ.** Interneuron and pyramidal cell interplay during in vitro seizure-like events. *J Neurophysiol* 95: 3948–3954, 2006.